Photoinduced Charge Transfer Dissociation of Al⁺−Ethene, −Propene, and −Butene

W.-Y. Lu, R.-G. Liu, T.-H. Wong, J. Chen, and P. D. Kleiber*

Department of Physics and Astronomy and Optical Science and Technology Center, University of Iowa, Iowa City, Iowa 52242

We have studied the photodissociation spectroscopy of weakly bound Al⁺−alkene bimolecular complexes (−ethene, −propene, and −butene) in the 216−320 nm spectral region. Molecular absorption bands are assigned to photoinduced charge transfer transitions to states that correlate with the $Al(3s^2 3p)$ + (alkene)⁺ product channels. Similarities in the absorption spectra for Al⁺−ethene, −propene, and −1-butene suggest similar equilibrium geometries with the metal ion lying above the alkene C=C π-bond in each case. The vibrational resonance structure is assigned to intramolecular modes of the alkene. The absorption spectra for Al⁺−2-butene are broader with less identifiable structure. A clear threshold for charge transfer dissociation to each alkene ion product gives a limit for the corresponding Al⁺−alkene bond dissociation energy: D_0''-(Al−X) ≤ 9.2, 19.1, 19.8, 24.7, and 28.2 kcal/mol for X = ethene, propene, 1-butene, *cis*-2-butene, and *trans*-2-butene, respectively. Experimental results are in good agreement with ab initio predictions.

I. Introduction

The interactions of metal ions with hydrocarbons are important in wide ranging areas of chemistry including heterogeneous and homogeneous catalysis, organometallic chemistry, and biochemical processes. Consequently, tremendous effort has gone into investigating bimolecular metal ion−hydrocarbon reaction mechanisms and energetics.[1−5] Detailed information about the structure and bonding of metal ion−hydrocarbon complexes is also important for developing a fuller understanding of chemical processes at metal ion catalytic centers. In this effort mass-resolved photodissociation spectroscopy of isolated molecular clusters has proven to be a valuable tool for probing the structure and chemical interactions of metal ion−hydrocarbon complexes under gas phase conditions.[6−9]

We have previously reported on the photodissociation spectroscopy of a series of light metal ion−ethene clusters, M⁺-(C₂H₄) with M = Mg, Ca, Zn, and Al.[10−13] Each bimolecular complex is weakly bound in a C_{2v} π-bonding geometry with the metal ion lying above the plane of the ethene ligand. For the group II metal ions (Mg, Ca, and Zn), the dominant absorption features correspond to metal-based excitations that correlate with the metal ion s−p resonance transitions.[10−12] However, for Al⁺−ethene the $Al^+(3s3p \leftarrow 3s^2)$ resonance lies at much higher energy (~7.42 eV) and the metal-centered band is not accessible for excitation wavelengths >220 nm. Rather, the near UV absorption spectrum is dominated by photoinduced charge transfer to excited states of the complex that correlate asymptotically with $Al(3s^2 3p)$ + C₂H₄⁺ product channels.[13] Typically, such metal ion−hydrocarbon charge transfer processes result in a fast dissociation and exhibit broad and structureless absorption bands.[14] The absorption spectrum for Al⁺(C₂H₄), however, shows three molecular bands that are assigned as 1^1B_2, 1^1B_1, and $2^1A_1 \leftarrow 1^1A_1$, corresponding to the three different symmetry alignments of the Al neutral ground state p-orbital with respect to the intermolecular bond axis. These excited states exhibit distinctly different molecular orbital interactions with the ethene ligand, giving useful insight into the Al−ethene charge transfer interactions. Of these excited states, 1^1B_1 is found to be long-lived, and the absorption band shows pronounced vibrational structure corresponding to excitation of both intermolecular and intramolecular vibrational motions.

Here we extend these studies of charge transfer interactions to the larger alkenes, propene and butene. We are particularly interested in determining how the complex structure, bonding, and charge transfer dynamics might be affected by the change in size and complexity of the alkene ligand. We will focus on the Al⁺ clusters with ethene, propene, and 1-butene that show similar spectral absorption features, reflecting similar bonding and interactions. We will only briefly discuss the spectroscopy of Al⁺−2-butene clusters that show very different spectroscopic structure.

II. Experimental Arrangement

The experimental apparatus and its application in mass-selected cluster photodissociation experiments has been previously described so only a brief overview will be given here.[9−13] Weakly bound Al⁺(alkene) complexes are produced in the supersonic molecular beam expansion from a standard transverse laser vaporization source. The supersonic expansion is initiated by a gas pulse of mixed alkene (5% ethene, propene, or butene) in Ar carrier gas from a pulsed supersonic valve operated at a backing pressure of ~40 psi. Alkene samples of 99+% purity were obtained from Aldrich and used without further purification. Downstream from a molecular beam skimmer, ionic clusters are pulse-extracted and accelerated into the flight tube of an angular reflectron time-of-flight mass spectrometer. The target cluster is mass-selected by a pulsed mass-gate and probed in the region of the reflectron with a Nd:YAG pumped tunable optical parametric oscillator (Spectral-Physics MOPO-SL) with frequency doubling capabilities. The laser band width is ≤0.15 cm⁻¹. Parent and daughter ions are then reflected to an off-axis microchannel plate detector in a standard tandem time-of-

* To whom correspondence should be addressed. Fax: (319)-335-1753. E-mail: paul-kleiber@uiowa.edu.
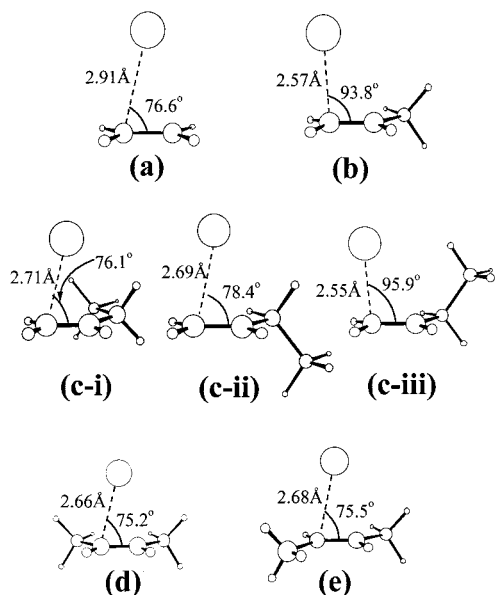
Figure 1. Optimized Al⁺−alkene complex geometries: (a) −ethene; (b) −propene; (c) −1-butene; (d) −*cis*-2-butene; (e) −*trans*-2-butene.

TABLE 1: Al⁺−Alkene Bond Dissociation Energies (kcal/mol)

alkene	D_0'' (experimental)[a]	D_e'' (theoretical)
ethene	9.2, 13 ± 2[b]	12.7
propene	19.1	18.1
1-butene	19.8	19.6, 19.2, 19.0[c]
cis−2-butene	24.7	21.8
trans−2-butene	28.2	21.2

[a] Uncertainty in the spectral threshold is <0.5 kcal/mol. These threshold values represent an upper limit to the actual bond energy. [b] From ref 16. [c] Values are given for the three stable π-bonded isomers as discussed in the text.

flight arrangement. Digital oscilloscopes and a multichannel scaler are used to monitor the mass spectrum. Integrated daughter ion signals are collected as a function of laser wavelength with a set of gated integrator channels, interfaced to a laboratory personal computer for data analysis.

The overall photofragmentation action spectrum is determined by measuring the integrated daughter ion signals as a function of photolysis laser wavelength, normalized by the parent ion signal and laser intensity. The major products observed in every case are Al⁺ and the corresponding alkene ion charge transfer product. The photofragment signals are verified to be linear over the range of laser pulse energies used in this work, consistent with a one-photon dissociation process.

III. Results and Discussion

A. Electronic Structure Calculations. We have carried out ab initio electronic structure calculations for the Al⁺−alkene complexes (−ethene, −propene, and −butene) using the *Gaussian '94* software package.[15] In each case ground state optimization calculations at the QCISD(T)//MP2/6-311++g(2d,p) level find a weakly bound singlet ground state in an equilibrium geometry with Al⁺ lying above the C=C π-bond of the alkene. Equilibrium structures are shown in Figure 1 and binding energies are summarized in Table 1. For Al⁺−C₂H₄ (Figure 1a) the metal ion lies above the bond midpoint in C_{2v} symmetry with an equilibrium bond distance (measured to the terminal carbon atom) of R_{Al-C} = 2.91 Å, an Al−C=C bond angle of 76.6°, and a bond-dissociation energy of D_e''(Al−C₂H₄) = 12.6
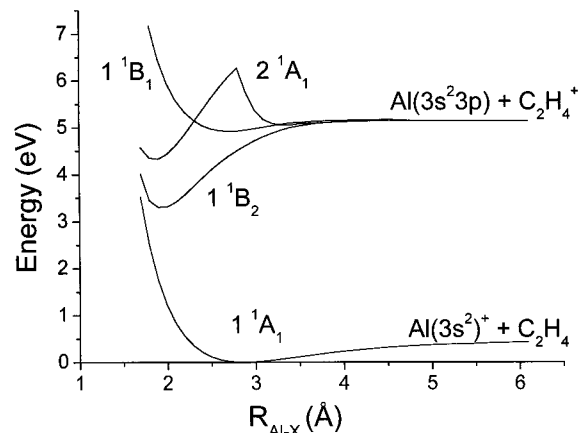
Figure 2. Low-lying singlet states of Al⁺(C₂H₄). Calculational details are given in ref 13.

kcal/mol. The ethene moiety shows only a slight out-of-plane distortion, and the calculated C−C bond length (R_{C-C} = 1.342 Å) is close to the experimental bond length for isolated ethene (1.337 Å), consistent with the weakly bound nature of the complex.[13]

For Al⁺−C₃H₆ (Figure 1b) the metal ion again lies above the C=C π-bond, but off-center, closer to the terminal carbon atom. Stronger binding is found for Al⁺−propene, which has an equilibrium intermolecular bond distance (measured to the terminal carbon atom) of R_{Al-C} = 2.57 Å and an Al−C=C bond angle of 93.8°. The bond-dissociation energy is D_e''(Al−C₂H₄) = 18.1 kcal/mol.

For Al⁺−1-butene there are three stable isomers, as shown in Figure 1c(i)−(iii), differing essentially in the orientation of the terminal methyl group with respect to the Al−butene intermolecular bond. In the most stable isomer (Figure 1c(i)) the C−C chain lies in a plane, with Al⁺ above the C=C π-bond and close to the midpoint, as in Al⁺−C₂H₄. For this isomer the equilibrium intermolecular bond distance (measured to the terminal carbon atom) is R_{Al-C} = 2.71 Å, with an Al−C=C bond angle of 76.1°, and a bond-dissociation energy of D_e''-(Al−C₂H₄) = 19.6 kcal/mol. However, the distinct isomers of Figures 1c all have very similar binding energies. For the trans form of Al⁺−1-butene shown in Figure 1c(ii), the binding energy is 19.2 kcal/mol, while for the cis form of Figure 1c(iii) the binding energy is 19.0 kcal/mol. We have explored the potential energy surface as a function of the dihedral angle of the terminal methyl carbon and find a barrier of ∼3 kcal/mol for isomerization. The clusters in our supersonic molecular beam expansion are expected to be relatively cold, and this barrier is probably too high to allow the methyl group to readily "flip" between these isomeric forms. However, it is likely that all three isomers are formed in the laser vaporization source and our spectroscopic results will then represent an average over the spectra for all three isomers. This will probably lead to a broadening of the observed spectrum for this complex.

We have also carried out similar calculations for both Al⁺−*cis*-2-butene and Al⁺−*trans*-2-butene, and the results are also shown as Figures 1d−e. The theoretical binding energies are 21.8 and 21.2 kcal/mol, respectively. The general increase in binding energy with alkene size is likely due to the increasing polarizability of the hydrocarbon.

We have previously carried out ab initio calculations of the excited states of Al⁺(C₂H₄).[13] Potential energy curves for the four low-lying singlet states of the complex are reproduced in Figure 2 merely to help guide the discussion. The three lowest electronically excited states all have appreciable charge transfer

Charge Transfer Dissociation of Al$^+$−Alkenes

J. Phys. Chem. A, Vol. 106, No. 5, 2002 **727**

(CT) character and correlate to the Al (3s^{2}3p) + C$_2$H$_4$$^+$ asymptote at long range. Energy differences in the CT states result from the differing alignments of the neutral Al(3s^{2}3p) p-orbital with respect to the C=C π-bond of the ethene ion. In the deeply bound 1^{1}B$_2$ state, the p-orbital is aligned parallel to the C=C bond. In the weakly bound 1^{1}B$_1$ state it lies perpendicular to the Al−C−C plane. In the 2^{1}A$_1$ state, which is repulsive at long range, the Al p-orbital lies in the Al−C−C plane but perpendicular to the C−C bond. These ab initio results predict three distinct UV molecular absorption bands in the 200−300 nm range, in good agreement with experimental observations.[13]

B. Action Spectra. *1. Al$^+$−Ethene, −Propene, and −1-Butene.* Al$^+$ is the major photofragment observed, with the alkene ion product channel accessible only above a clear spectroscopic threshold in each of these Al$^+$−alkene complexes. The action spectra for dissociation to Al$^+$ from each of these complexes are remarkably similar, as shown in Figure 3. In each case there is evidence for three distinct absorption bands: a weak continuum band at longer wavelengths, a stronger band at intermediate wavelengths showing vibrational resonance structure, and a third incomplete continuum band at shorter wavelengths. The similarities in the absorption spectra indicate similar electronic structure, which in turn supports the conclusion based on ab initio calculations that the ground state equilibrium geometry of the complexes should be similar, with the Al$^+$ lying above the plane of the alkene C=C π-bond. The electronic absorption bands are then expected to be similar since the dominant molecular orbital interactions in the photoinduced charge transfer state involve the Al ground state p-orbital with the C=C π-orbitals of the alkene ligand, and these will be similar and relatively independent of the structure and complexity of the rest of the alkene molecule.

We have previously discussed the assignment of the absorption bands of Al$^+$−ethene.[13] (Figure 3a) The very weak, low energy continuum band of Al$^+$(C$_2$H$_4$) in the range 290−250 nm is assigned as 1^{1}B$_2$ ← 1^{1}A$_1$ in C$_{2v}$ symmetry. In this alignment the Al p-orbital can overlap with the π*-antibonding LUMO of ethene allowing for efficient transfer of electron density, which weakens and stretches the C=C bond. This is accompanied by formation of a partial Al−C−C σ-bond with a dramatic shortening of the Al−ethene bond length.[13] This bond stretch insertion process facilitates a nonadiabatic transition to the ground state through an avoided surface crossing conical intersection in A′ symmetry. Equivalently, the *in-plane* wag vibrational motion (of b$_2$ symmetry) in the ^{1}B$_2$ excited state can couple this state to the ^{1}A$_1$ ground state [B$_2$ ⊗ B$_2$ = A$_1$], allowing an efficient pathway for nonadiabatic quenching. The observed 1^{1}B$_2$ ← 1^{1}A$_1$ absorption band is a broad structureless continuum, as expected for a large geometry change. Ab initio calculations support the bond-stretch quenching mechanism. SCF level calculations find that the equilibrium geometry of the 1^{1}B$_2$ state of the complex shows significant insertion character with a considerable stretch in the C=C bond, accompanied by a dramatic shortening of the Al−ethene bond. We have also identified an accessible region of 1^{1}B$_2$(A′)−1^{1}A$_1$-(A′) surface crossing with substantial insertion character.[13]

The Al$^+$−propene and −1-butene complexes have a similar geometry with the metal ion lying above the plane of the C=C π-bond, although somewhat off-center, closer to the terminal C atom. On the basis of the similarities in the spectra, we assign the longer wavelength continuum bands in the range 308−270 nm for both Al$^+$−propene (Figure 3b) and Al$^+$−1-butene (Figure 3c) to the analogous photoinduced charge transfer
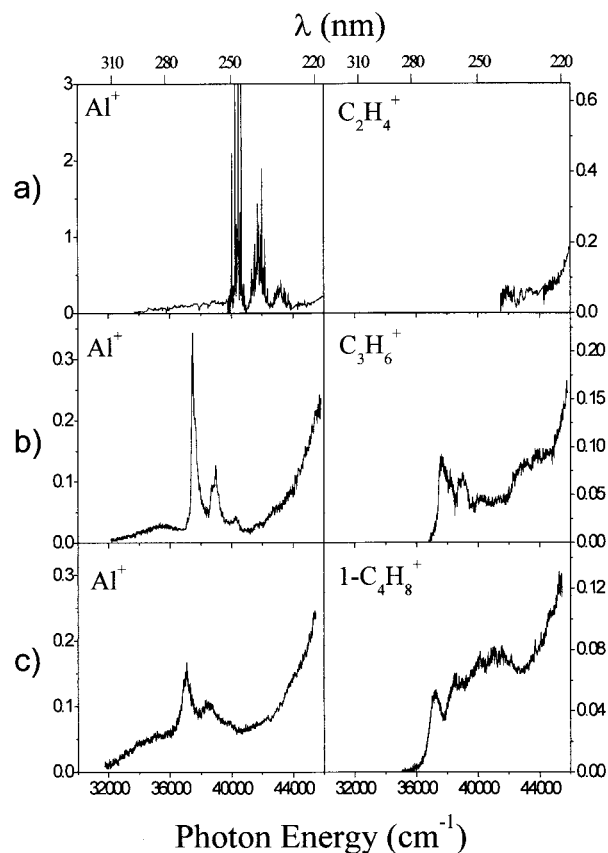

Figure 3. Action spectra for the photoinduced charge transfer dissociation of (a) Al$^+$−ethene (top panel), (b) Al$^+$−propene (center panel), and (c) Al$^+$−1-butene (bottom panel).

process, with the neutral ground state Al p-orbital aligned roughly parallel with the C=C π-bond of the alkene. Ab initio optimization calculations at the CIS level for the equilibrium geometry of the first excited state of Al$^+$−propene and Al$^+$−1-butene show that, following excitation, the complex relaxes by stretching the C=C bond and pulling the Al atom in and toward the center of the alkene π-bond. It is likely that, as in Al$^+$−ethene, this bond stretch process will facilitate coupling back to the ground state surface, leading to dissociation by reverse charge transfer and accompanied by significant vibrational excitation of the alkene. The photodissociation signal in this band is much stronger for both Al$^+$−propene and −1-butene than for Al$^+$−ethene. This is probably because the reduced symmetry and greater density of vibrational states allows for a more efficient coupling to the ground state surface.

The spectra of Figures 3 all show a sharp onset of vibrational resonance structure at intermediate energies. In Al$^+$−ethene we can clearly identify the vibrational origin (0$_0^0$ = 40 042 cm^{-1}) of the second excited electronic state, assigned as 1^{1}B$_1$. Because of limited molecular orbital overlap between Al p-orbital and the alkene ion LUMOs in this symmetry, the state is characterized by relatively weak binding interactions. The pronounced vibrational resonance structure of Figure 3a shows both low-frequency intermolecular vibrational motions and higher frequency intramolecular ethene vibrations. Vibrational assignments have been discussed in ref 13. The low-frequency modes are assigned to the Al−C$_2$H$_4$ a$_1$-intermolecular stretch (ν_2 = 230 cm^{-1}) and the Al−C$_2$H$_4$ b$_1$-intermolecular wag (ν_3 = 328 cm^{-1}). The assignment for the higher frequency modes at 1264 and 1521 cm^{-1} is not conclusive, but these are probably associated with the a$_1$ H−C−H bend and C=C stretch, respectively.[13] The observation of significant excitation in the

high-energy intramolecular vibrational modes of the hydrocarbon ligand is somewhat unusual. In metal-based transitions such modes are generally not strongly excited because the equilibrium geometry of the hydrocarbon does not drastically change on excitation of the metal ion chromophore. However, significant geometry changes are expected in this charge transfer process that effectively ionizes the ethene ligand within the complex.

Again, on the basis of the similarities in the spectra of Figure 3, we assign the structured intermediate energy band in Al^+- propene and −1-butene to the analogous transition with the Al p-orbital lying perpendicular to the $Al-C=C$ plane. The onset of vibrational structure (at ∼37 500 cm^{-1} for Al^+-propene and at ∼37 100 cm^{-1} for Al^+-1-butene) defines the energy minimum of the second excited electronic state in each case. These bands show a significant red-shift consistent with a stronger excited state binding for both Al^+-propene and −1-butene than for Al^+-ethene. The low-frequency vibrational structure is unresolved; however, we can clearly identify a second vibrational resonance peak in each case that lies roughly 1500 cm^{-1} above the origin and probably corresponds to excitation of one quantum of higher frequency intramolecular alkene vibration, either the $C=C$ stretch or $H-C-H$ bend, or both. Because the vibrational structure is not fully resolved, we are unable to precisely assign the band origin or mode frequencies. The increasing complexity of the vibrational resonance structure with the size of the alkene ligand is expected because of the lower symmetry and increasing density of states that allows for more efficient intramolecular vibrational mode coupling. There is an appreciable geometry change on excitation to the charge transfer state with the alkene ligand distorting toward the equilibrium geometry of the ion. Furthermore, in the case of Al^+-1-butene we are probably averaging over an ensemble of the three stable π-bonded isomers.

The Al^+-ethene absorption spectrum of Figure 3a shows a gradual increase at higher energies, corresponding to excitation of the $2^1A_1 \leftarrow 1^1A_1$ band. In this symmetry the Al metal ion p-orbital lies in the $Al-C=C$ plane, but perpendicular to the $C=C$ bond. The state is repulsive at long range but shows evidence for short-range chemical bonding due to mixing with higher lying states. A similar high-energy continuum above 42 000 cm^{-1} is seen in both Al^+-propene and −1-butene and is assigned to the analogous charge transfer transition in these complexes.

2. Al^+-2-Butene. The photodissociation spectra for both Al^+-cis-2-butene and $Al^+-trans$-2-butene are markedly different from the spectra for the other Al^+-alkene complexes described above. The absorption bands are much broader and show less identifiable structure. Figure 4 shows the spectrum for Al^+-cis-2-butene for comparison. The spectrum for $Al^+-trans$-2-butene is similar. The significant difference with Al^+-1-butene may be due to the closer proximity of the metal ion to the methyl groups in either the *cis*- or *trans*-2-butene complexes. Because of this proximity, the extended p-orbital of Al in the charge transfer state will more strongly interact with the methyl groups, leading to a larger electronic band shift and more significant distortion of the complex, resulting in greater vibrational excitation and a more complicated vibronic spectrum. It is also interesting to note that dissociation of Al^+-2-butene gives a small branching (∼5%) to the reactive product channel $AlCH_3 + C_3H_5^+$, resulting from $C-C$ σ-bond cleavage in the complex. This observation is consistent with the hypothesis that the Al metal atom strongly interacts with the methyl groups in the charge transfer state.
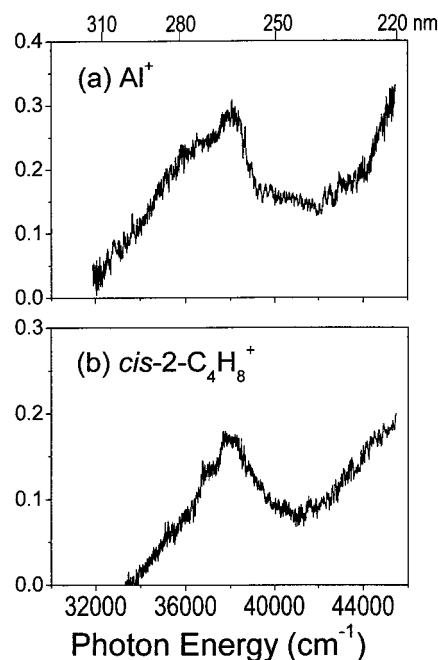

Figure 4. Action spectra for Al^+-cis-2-butene.

C. Bond Dissociation Energies. In each of the Al^+-alkene complexes studied, there is a spectroscopic threshold for dissociation to the alkene ion charge transfer product. These threshold values can be used to place an upper limit on the ground state bond dissociation energy through the energy cycle:[14]

$$D_0''(\text{Al}-\text{alkene}) \leq h\nu_{\text{threshold}} - [\text{IP(alkene)} - \text{IP(Al)}] \quad (1)$$

Results are summarized in Table 1.

For Al^+-ethene the spectroscopic threshold is difficult to determine. (Figure 3a) The $C_2H_4^+$ signal rises very weakly and slowly from $\lambda \sim 252$ nm, over a long range of energies. Because the signal is weak at longer wavelengths, it is not possible to carry out the usual experimental linearity tests in the region 227 nm $< \lambda <$ 252 nm. For $\lambda \leq 227$ nm the observed $C_2H_4^+$ signal is linear in laser power. Above the energetic threshold, the $C_2H_4^+$ product action spectrum appears as a weak continuum; relative branching to the $C_2H_4^+$ product increases with photolysis energy, approaching 50% at the shortest wavelengths accessible in these experiments.

Assuming a threshold wavelength of $\lambda = 252 \pm 1$ nm (4.92 $\pm$ 0.02 eV), we estimate the $Al^+-C_2H_4$ bond dissociation energy (BDE) by

$$D_0''(\text{Al}-\text{ethene}) \leq 4.92 - [10.51 - 5.99] =$$
$$0.40 \pm 0.02 \text{ eV} = 9.2 \pm 0.5 \text{ kcal/mol}$$

For Al^+-ethene we were also able, in our previous work, to obtain an independent estimate for the bond dissociation energy from the measured translational energy release in the CT dissociation channel at higher photolysis energies.[13] The observed maximum total kinetic energy release at 218 nm was used to estimate the $Al^+-C_2H_4$ binding energy:

$$D_0''(\text{Al}^+-\text{ethene}) = h\nu - \text{KER} - [\text{IP}(C_2H_4^+) - \text{IP(Al)}]$$

The result, $D_0''(\text{Al}^+-C_2H_4) = 0.4 \pm 0.2$ eV, is in good agreement with the threshold measurement, although the relative uncertainty is large.

Our limit on the experimental bond energy from the spectroscopic threshold for $C_2H_4^+$ production, $D_0''(\text{Al–ethene}) \leq$ 9.2 kcal/mol (0.40 eV), is appreciably lower than the value of $D_e''(\text{Al}^+-\text{ethene}) = 13 \pm 2$ kcal/mol reported by Stöckigt et al.[16] This value was obtained from a combination of ab initio quantum chemical theoretical methods and experimental kinetic equilbrium measurements using Fourier transform ion cyclotron mass spectrometry and bracketing techniques. The difference is somewhat outside the combined error bars. Zero point energy corrections are expected to be small ∼0.7 kcal/mol and will not fully resolve this difference. Rotational line shape data for the origin band gives a rotational temperature <30 K for the clusters in our apparatus, and the vibrational spectrum shows no evidence for any hot band absorption. Thus, it appears unlikely that the discrepancy results from dissociation of vibrationally hot clusters from the source. The origin of this discrepancy is not yet understood.

For Al⁺−propene and −butene, the spectroscopic thresholds for the corresponding alkene ion product channels are much more clear and sharp (Figure 3b,c). The threshold for Al⁺−propene lies at $\lambda = 271.5 \pm 1$ nm (4.57 ± 0.02 eV), leading to a bond dissociation energy of $D_0''(\text{Al–propene}) \leq 19.1 \pm 0.5$ kcal/mol.

The corresponding ab initio value is $D_e'' = 18.1$ kcal/mol at the QCISD(T)//MP2/6-311++g(2d,p) level. Similarly, the threshold for Al⁺−1-butene lies at $\lambda = 280 \pm 1$ nm, leading to a bond dissociation energy of $D_0''(\text{Al–1-butene}) \leq 19.8 \pm 0.5$ kcal/mol with a corresponding ab initio value of $D_e'' = 19.6$ kcal/mol for the most stable isomer (Figure 1c(i)). The experimental bond energies for the larger clusters are in quite good agreement with ab initio results. (This makes the limited agreement for the case of Al⁺−ethene even more perplexing.) We have used analogous threshold measurements to obtain upper limits on the bond energies for Al⁺−*cis*-2-butene and Al⁺−*trans*-2-butene and the results are also summarized in Table 1.

Finally, it is interesting to note that our experimental spectroscopic results imply a long-range barrier to dissociation on the charge transfer state surface for each of the Al⁺−alkene clusters with ethene, propene, and 1-butene. In each case, vibrational resonance structure is observed at energies well above the threshold for charge transfer dissociation to the alkene ion product. Indeed, homogeneous lifetime broadening due to this charge transfer dissociation channel may contribute to the lack of resolvable vibrational resonance structure.

MCSCF excited state potential energy calculations for Al⁺−ethene do indeed show a barrier in the 1^1B_1 state, near $R_{\text{Al}-X} \sim$ 3.2 Å, with a height above the CT asymptote estimated as 0.4 eV.[13] We expect that more sophisticated calculations (that allow for relaxation of the ethene ion) will show a higher long-range barrier to dissociation on the 1^1B_1 surface, consistent with these experimental observations. A similar barrier may also be expected for Al⁺−propene and −1-butene.

For each of these Al⁺−alkene clusters, the relative branching to the alkene ion channel increases above the threshold for charge transfer dissociation. Evidently, Franck−Condon excitation from the ground state equilibrium can access regions of the excited state surfaces that allow a channel for direct CT dissociation, but direct CT dissociation competes with nonadiabatic quenching and reverse CT to Al⁺ products.

IV. Conclusions

We have reported on the photodissociation spectroscopy of weakly bound Al⁺−alkene bimolecular complexes (ethene,

propene, and 1-butene) in the 216−320 nm spectral region. For each cluster three molecular absorption bands are observed and assigned to photoinduced charge transfer transitions to states that correlate with the $\text{Al}(3s^23p)$ + (alkene)⁺ product channels. Similarities in the absorption spectra suggest similar equilibrium geometries with the metal ion lying above the alkene C=C π-bond in each case. The electronic absorption bands are expected to be similar in this case since the dominant molecular orbital interactions involve the Al neutral p-orbital with the alkene ion C=C π-bond in each case and will be relatively independent of the structure and complexity of the rest of the alkene molecule. Vibrational resonance features are assigned to intramolecular modes of the alkene ligand, probably the H−C−H bend and the C=C stretch. Excitation of these modes is expected in the charge transfer transition that effectively ionizes the alkene ligand in the complex. A clear threshold for charge transfer dissociation to the alkene ion product allows us to place a limit on the Al⁺−alkene bond dissociation energy: $D_0''(\text{Al}-X) \leq$ 9.2, 19.1, and 19.8 kcal/mol for X = ethene, propene, and 1-butene, respectively. These experimental results are in good agreement with ab initio predictions.

The absorption spectra for Al⁺−*cis*-2-butene and Al⁺−*trans*-2-butene are markedly different, being much broader and showing less identifiable structure. This is probably due to the close proximity between the metal atom and the methyl groups in the charge transfer state of these complexes, resulting in larger electronic band shifts and more significant distortion of the complex. Charge transfer threshold measurements give the bond dissociation energies as $D_0''(\text{Al}-X) \leq$ 24.7 and 28.2 kcal/mol for X = *cis*-2-butene and *trans*-2-butene, respectively.

References and Notes

(1) Eller, K.; Schwarz, H. *Chem. Rev.* **1991**, *91*, 1121.

(2) Armentrout, P. B. *Acc. Chem. Res.* **1995**, *28,* 430. Armentrout, P. B. In *Selective Hydrocarbon Activation: Principles and Progress*; Davies, J. A., Watson, P. L., Liebman, J. F., Greenberg, A., Eds.; VCH: New York, 1990.

(3) Weisshaar, J. C. *Acc. Chem. Res.* **1993**, *26,* 213. Weisshaar, J. C. *Adv. Chem. Phys.* **1992**, *82,* 213.

(4) Van Koppen, P. A. M.; Kemper, R. R.; Bowers, M. T. In *Organometallic Ion Chemistry*; Freiser, B. S., Ed.; Kluwer Academic Press: Boston, 1996.

(5) Freiser, B. S. *Acc. Chem. Res.* **1994**, *27*, 353. Freiser, B. S. *J. Mass Spectrom.* **1996**, *31,* 703.

(6) Pilgrim, J. S.; Yeh, C. S.; Willey, K. F.; Robbins, D. L.; Duncan, M. A. *Int. Rev. Phys. Chem.* **1994**, *13*, 231. Duncan, M. A. *Annu. Rev. Phys. Chem.* **1997**, *48,* 69.

(7) Farrar J. M. In *Cluster Ions*; Ng, C. Y., Baer, T., Powis, I., Eds.; Wiley: New York, 1993; p 243.

(8) Lessen, D. E.; Asher, R. L.; Brucat, P. J. In *Advances in Metal and Semiconductor Clusters*; Duncan, M. A, Ed.; JAI Press: Greenwich, CT, 1983; Vol. I, p 267. Lessen, D. E.; Asher, R. L.; Brucat, P. J. *Int. J. Mass Spectrom. Ion Processes* **1990**, *102,* 331.

(9) Kleiber, P. D.; Chen, J. *Int. Rev. Phys. Chem.* **1998**, *17,* 1.

(10) Chen, J.; Wong, T. H.; Montgomery, K.; Cheng, Y. C.; Kleiber, P. D. *J. Chem. Phys.* **1998**, *108,* 2285.

(11) Holmes, J. H.; Kleiber, P. D.; Olsgaard, D. A.; Yang, K. H. *J. Chem. Phys.* **2000**, *112,* 6583.

(12) Lu, W. Y.; Yang, K. H.; Kleiber, P. D.; Young, M. A. *J. Chem. Phys.* **2001**, *115,* 5823.

(13) Chen, J.; Wong, T. H.; Kleiber, P. D.; Yang, K. H. *J. Chem. Phys.* **1999**, *110*, 11798.

(14) Willey, K. F.; Yeh, C. S., Robbins, D. L.; Duncan, M. A. *J. Phys. Chem.* **1992**, *96,* 9106. Willey, K. F.; Cheng, P. Y.; Pearce, K. D.; Duncan, M. A. *J. Phys. Chem.* **1990**, *94,* 4769. Willey, K. F.; Cheng, P. F.; Bishop, M. B.; Duncan, M. A. *J. Am. Chem. Soc.* **1991**, *113*, 4721.

(15) Frisch, M. J.; Trucks, G. W.; Schlegel, H. B.; Gill, P. M. W.; Johnson, B. G.; Robb, M. A.; Cheeseman, J. R.; Keith, T.; Petersson, G. A.; Montgomery, J. A.; Raghavachari, K.; Al-Laham, M. A.; Zakrzewski, V. G.; Ortiz, J. V.; Foresman, J. B.; Cioslowski, J.; Stefanov, B. B.; Nanayakkara, A.; Challacombe, M.; Peng, C. Y.; Ayala, P. Y.; Chen, W.; Wong, M. W.; Andres, J. L.; Replogle, E. S.; Gomperts, R.; Martin, R. L.; Fox, D. J.; Binkley, J. S.; Defrees, D. J.; Baker, J.; Stewart, J. P.; Head-Gordon, M.; Gonzalez, C.; Pople, J. A. *Gaussian 94*, revision D.4; Gaussian, Inc.: Pittsburgh, PA, 1995.

(16) Stoeckigt, D.; Schwarz; J.; Schwarz, H. *J. Phys. Chem.* **1996**, *100*, 8786.